Minority Carrier Traps Induced by Neutron Reactions with 4H-SiC

Author(s):
Belanche Guadas, Manuel; Bathen, Marianne Etzelmüller; Kumar, Piyush; Dorfer, Christian; Martinella, Corinna; Grossner, Ulrike

Publication date:
2023

Permanent link:
https://doi.org/10.3929/ethz-b-000640705

Originally published in:
Defect and diffusion forum 426, https://doi.org/10.4028/p-724d7y

Defect and Diffusion Forum
ISSN: 1662-9507, Vol. 426, pp 23-28
doi:10.4028/p-724d7y

Submitted: 2022-09-04
Revised: 2023-01-18
Accepted: 2023-01-18
Online: 2023-06-06

Minority Carrier Traps Induced by Neutron Reactions with 4H-SiC

Manuel Belanche[1,a*], Marianne E. Bathen[1,b], Piyush Kumar[1,c], Christian Dorfer[1,d], Corinna Martinella[1,e], and Ulrike Grossner[1,f]

[1]Advanced Power Semiconductor Laboratory, ETH Zürich, Physikstrasse 3, 8092 Zürich, Switzerland

[a]belanche@aps.ee.ethz.ch, [b]bathen@aps.ee.ethz.ch, [c]kumar@aps.ee.ethz.ch, [d]dorfer@aps.ee.ethz.ch, [e]martinella@aps.ee.ethz.ch, [f]ulrike.grossner@ethz.ch

Keywords: Neutron Irradiation, Neutron Damage, MCTS, Point Defects, 4H-SiC

Abstract. This work presents the characterization of minority carrier traps in epitaxial n-type 4H-SiC after high fluence neutron irradiation using minority carrier transient spectroscopy (MCTS) in a temperature range of 20 K to 660 K. Three minority carrier trap levels are reported, labelled as X, B and Y, whose activation energies were estimated by Arrhenius analysis and where the B level is assigned to substitutional boron (B_{Si}). The dynamic behaviour of the trap levels was studied by consecutive temperature scans.

Introduction

Silicon carbide (SiC) devices are a well-established technology in the high-power electronics industry [1]. Owing to its wide band gap, radiation hardness, and high melting point, SiC is also drawing the attention from the aerospace industry [2] as well as nuclear reactor facilities as a promising material for radiation detectors [3]. However, the adoption of SiC in these applications is held back by the interaction of the devices with their radiation environment which needs to be further studied and understood to comply with quality and reliability requirements. The energetic particles present in such kind of environments can create electrically active defects causing the deterioration in device performance. In fact, through inelastic scattering and nuclear reactions, particles can induce defects in the crystal which can cause destructive single-event effects in power devices, i.e., single-event burnout (SEB) and single-event gate rupture (SEGR) [4, 5], as well as degrading the sensitivity of SiC detectors. This is the case for the interactions of SiC devices with energetic neutrons. The present work focuses on the interplay between energetic neutrons and SiC material and the electrically active defects formed by this kind of interaction.

Characterization and identification of the defects created in SiC material and devices by neutrons is crucial for the improvement of radiation hardness of SiC devices. Furthermore, a thorough understanding of the complex interactions occurring between the neutrons and the material is vital when investigating the viability of fabrication processes like neutron transmutation doping (NTD) in SiC, which is widely used for silicon due to its superior uniform dopant concentration [6].

The nature of defects in the 4H-SiC crystal acting as minority and majority charge carrier traps has been extensively studied, however, several open questions remain, particularly in the case of the dependence of minority carrier traps on irradiation and annealing. The most dominant majority carrier traps that are typically found even in state-of-the-art n-type 4H-SiC epitaxial layers [7] are the $Z_{1/2}$ and $EH_{6/7}$ levels. They have been assigned to the double acceptor state transition (2-/0) and to the double donor state transition (2+/+/0) of the carbon vacancy (V_C), respectively [8]. Other commonly observed deep levels after irradiation are S1/S2 and EH1/EH3 with activation energies of $E_a = 0.4\,\text{eV}$ and $E_a = 0.7\,\text{eV}$ below the conduction band edge (E_C) [9]. These levels can be created with neutron irradiation [10]. Recent work has shown that EH1/EH3, or the EH-center, are carbon interstitial (C_i) related defects [11]. The S1/S2 levels, or the S-center, have a very similar energy position in the band gap but have been associated to the silicon vacancy (V_{Si}) [12].

Compared to majority carrier traps, minority carrier traps in 4H-SiC are much less explored. Two minority trap levels have been reported and are usually labelled as B- and D-center, with estimated activation energies of $E_a = 0.27\,eV$ and $E_a = 0.60\,eV$ above the valence band edge (E_V). While the B-center is ascribed to substitutional boron at a silicon site (B_{Si}) [13], the nature of the D-center is still unclear. The reported results are debating between its association with a substitutional boron at carbon site (B_C) or to a B_{Si} next to a carbon vacancy (V_C).

The goal of this study is to further investigate the influence of neutron irradiation on the minority carrier traps of SiC. To do so, n-type 4H-SiC epitaxial layers were exposed to energetic neutrons to form defects in the material. Then, Schottky barrier diodes were formed on the irradiated 4H-SiC epi-layers and characterized by means of minority carrier transient spectroscopy (MCTS).

Experimental Details

Neutron irradiation. 4H-SiC samples of $10 \times 10\ mm^2$ with an n-type epitaxial layer of $10\ \mu m$ thickness and a nitrogen doping concentration of $4 \times 10^{15}\ cm^{-3}$ were irradiated with neutrons at the Jozef Stefan Institute (JSI) TRIGA Mark II Reactor in Ljubljana, Slovenia. The neutron spectrum of channel F-19 of the reactor is shown in Fig. 1. Two peaks are observed in the neutron lethargy, one for thermal neutrons at 5.5×10^{-8} MeV and one for fast neutrons at $2\,MeV$. The selected neutron fluence was $1 \times 10^{15}\ cm^{-2}$. Gamma-ray spectroscopy measurements were performed 22 hours after the end of the irradiation to identify the active isotopes in the samples.

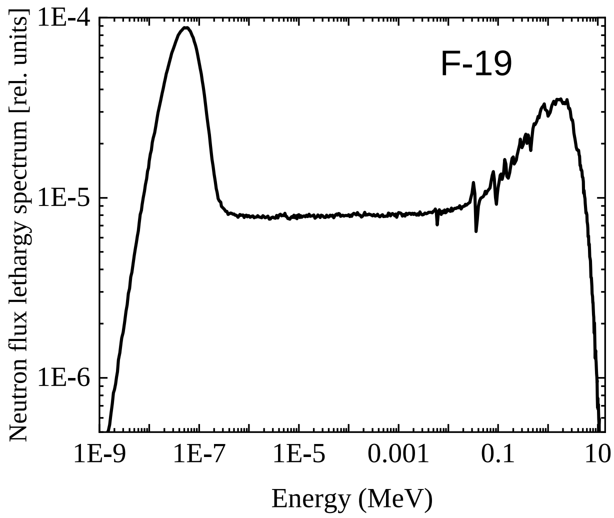

Fig. 1: Neutron spectra of channel F-19 at the Jozef Stefan Institute (JSI) TRIGA reactor [14].

4H-SiC samples. N-type Schottky barrier diodes were created on the irradiated 4H-SiC samples (N1 and N2), as well as on as-grown 4H-SiC pristine samples. Two layers of Ni were deposited to create the Schottky contacts, including one of $100\,nm$ thickness with a diameter of $0.8\,mm$ on top of a $20\,nm$ thickness and $2\,mm$ diameter layer. The latter behaves as a semi-transparent contact required for the optical excitation of carriers during MCTS measurements.

DLTS and MCTS measurements. In order to study the neutron-induced defects, deep level transient spectroscopy (DLTS) and minority carrier transient spectroscopy (MCTS) were performed. The deep level and minority carrier transient Fourier spectroscopy measurements were conducted using a High Energy Resolution Analysis Deep Level Transient Spectroscopy (PhysTech HERA-DLTS [15]) setup. The high neutron fluence induced enough defects to compensate the free electrons in the n-type 4H-SiC. This results in a flat DLTS spectrum and hinders the analysis of the defect induced trapping effects in the upper half of the band gap. Therefore, the focus of this study is on the minority carrier trap levels. During MCTS measurements, a $365\,nm$ LED was used at a power of $200\,mW$ and a pulse duration of $100\,ms$. A reverse bias of $-10\,V$ was applied during the measurement and consecutive temperature scans were carried out in several steps. The first scan was performed from 20 to $300\,K$, increasing the upper limit by $50\,K$ in the subsequent steps until $660\,K$ was reached. The MCTS signals presented refer to the coefficient of the sine term (b_1) in the Fourier series with a period width (T_W) of 200 ms. Although the optical pulsing scheme is designed for detecting the capture and emission of minority carriers (holes for the present case), majority carrier traps can also be detected if not all electrons are swept out of the depletion region by the applied reverse bias. Electron traps emerge in the MCTS spectrum as peaks with opposite sign, where positive and negative peaks correlate to electron and hole traps, respectively, for n-type material (see Fig. 2). Arrhenius analysis was performed on the observed peaks which allows the calculation of the electron or hole activation energy and measured capture cross section from the slope and intercept, respectively, of the Arrhenius plot of $\log(e_{n,p}/T^2)$ versus $1000/T$, where $e_{n,p}$ denotes the electron and hole emission rate and T the temperature.

Results and Discussion

Fig. 2 shows a comparison of the MCTS spectra for a temperature range of 20 K to 660 K between a neutron-irradiated (red solid curve) and an as-grown (black dotted curve) 4H-SiC sample. Several peaks were detected in both the as-grown and the irradiated samples. Regarding the former, a contribution from majority carriers is observed in the positive peak labelled as N at ~40 K. The N peak is related to the nitrogen [16] used for donor doping in SiC devices. The second peak, labelled as B, agrees with the reported shallow B-center [13] assigned to substitutional boron at a silicon site (B_{Si}). Its maximum is found at ~120 K in the pristine sample and its signature is $E_a = 0.25$ eV above the valence band edge according to Arrhenius analysis.

After the neutron irradiation, the same N peak is still observed at 40 K. However, a decrease in the peak magnitude can be observed, possibly due to the compensation of carriers caused by the defect traps created by the neutrons. In addition, three negative peaks labelled X, B and Y appear (see Fig. 2). Regarding the first peak, measured at 51 K, no information about a similar contribution was found in literature, therefore it was given the name X. Although further investigation into the nature of the peak is needed, an activation energy of $E_a = 0.06$ eV above the valence band maximum (VBM) was extracted from Arrhenius analysis, indicating that the defect may have a shallow dopant-like behavior. The deeper-lying Y level at ~575 K was assigned to an activation energy of $E_a = 1.6$ eV above the VBM and, similarly to the X level, no equivalent was found in literature. Clearly, neutron irradiation induces new defects acting as charge carrier traps with energy levels in the lower half of the band gap. These electrically active defects could have a detrimental impact on SiC devices and contribute to a lower radiation hardness.

Finally, the highest intensity peak observed in the MCTS was attributed to the B-center. The extracted activation energy was $E_a = 0.22$ eV above the VBM – similar to the boron peak found in the pristine sample. However, with respect to the pristine spectrum, the peak intensity is substantially increased, and the peak position appears to be shifted towards lower temperatures as compared to the as-grown case.

Gamma spectroscopy measurements performed after the neutron irradiation showed strong nuclear activation due to the interaction of high energy neutrons with the trace elements present in commercial 4H-SiC wafers. The correlation of these peaks and the impurities in the crystal is currently under investigation.

A second sample named N2 and irradiated at the same conditions (1×10^{15} cm^{-2} neutron fluence) also underwent MCTS analysis with double temperature sweep: ascending from 20 K to 660 K and descending from 660 K to 20 K; the latter shown in Fig. 3. A shift of 34 K towards lower temperature is measured for both irradiated samples (N1 and N2) for the shallow B peak, most likely due the increase of tensile stress in the crystal because of damage creation. A similar shift of the peak towards lower temperatures after neutron irradiation was previously reported by I. Capan *et. al.* [17]. In this case, a shift of roughly 15 K was observed between irradiation with an order of magnitude difference in fluence (from 1×10^{12} cm^{-2} to 1×10^{13} cm^{-2}). In the present study, a shift of 34 K is observed for a fluence of 1×10^{15} cm^{-2} as compared to an as-grown sample, which matches with the trend indicated

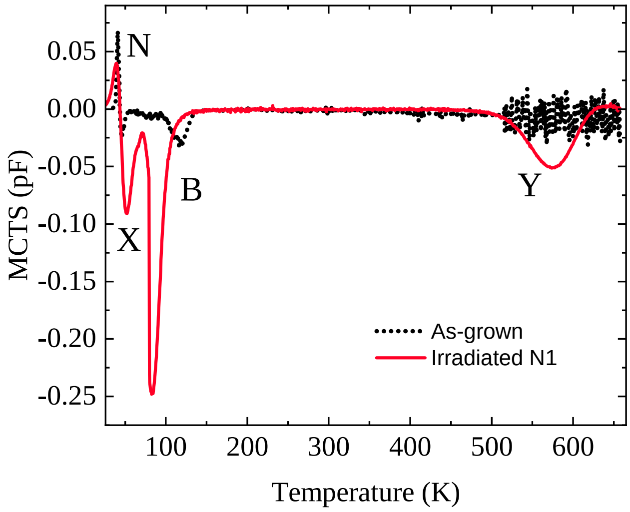

Fig. 2: MCTS spectra of the N1 sample (red-solid) irradiated with a total neutron fluence of $1 \times 10^{15}\,\mathrm{cm}^{-2}$ and an as-grown sample (black-dotted).

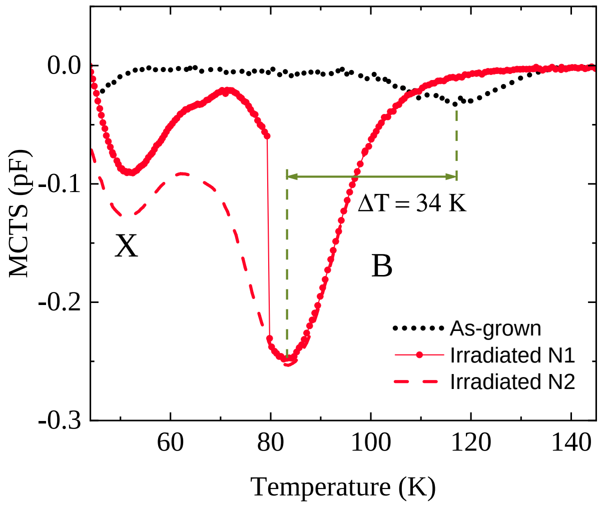

Fig. 3: MCTS spectra showing the X and B trap levels of N1 (red-scatter-line) and N2 (red-dashed), irradiated with $1 \times 10^{15}\,\mathrm{cm}^{-2}$ neutron fluence, and the as-grown sample (black-dotted). Zoom in the last scan of N1 (20 K to 660 K) and the descending scan of N2 (660 K to 20 K).

in Ref. [17]. The signal of the B-level in sample N1 shows a slightly skewed peak in its rising part. This was tentatively attributed to a short loss of contact during the temperature sweep (emphasized in Fig. 3 with the scatter-line curve), although further investigation is required.

In order to study the dynamic behaviour of the trap levels created, progressive temperature sweeps were performed, increasing the temperature by 50 K per step, as shown in Fig. 4 for the 25 K to 140 K temperature range (sample N1). Two effects can be observed; (i) a shift of the B peak along the x-axis towards lower temperature, and (ii) the peak intensities of the X and B peaks change between the runs. The response to the consecutive sweeps of the X-level and the B-level is shown in Fig. 4. Interestingly, both follow the same trend which could be a hint of a possible correlation that needs further investigation. The height of the peaks start by decreasing in magnitude until the 20 K to 600 K sweep, when it sets on an increasing trend. However, the B-level seems to have a stronger reaction once higher temperatures are reached, with an increase in peak intensity of 0.2 pF, whereas the X peak shows a rise of 0.07 pF. On the other hand, there is a shift of the maxima of 7 K to lower temperatures for the B-level while the X-level remains stable.

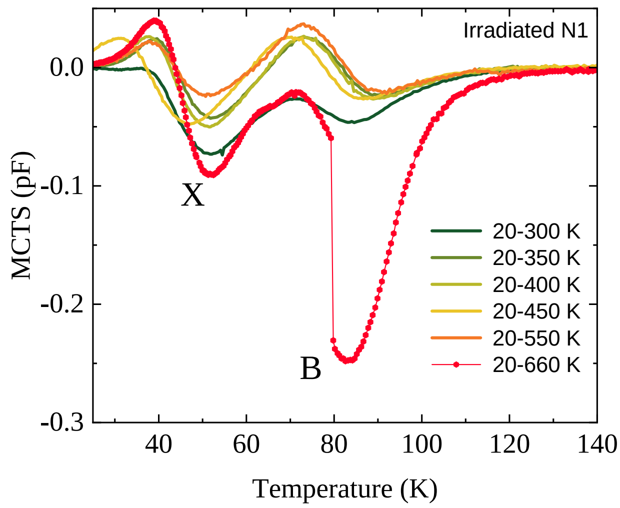

Fig. 4: MCTS spectra of consecutive temperature scans showing the dynamic behaviour of the X and B trap levels in the neutron irradiated sample N1.

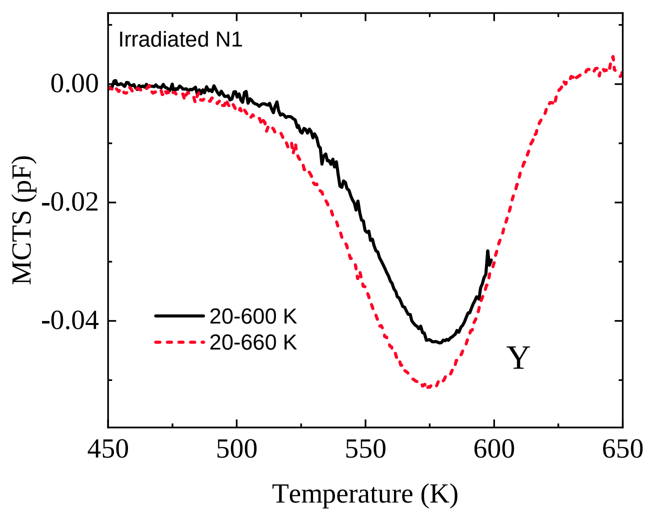

Fig. 5: MCTS spectra of the last three temperature sweeps showing the dynamic behaviour of the Y trap level in the neutron irradiated sample N1.

Fig. 5 is focusing on the behaviour of the high temperature peak labelled Y for the same sample (sample N1). In this case, the two sweeps able to detect the Y peak are compared. Both the effects of peak shifting and intensity enhancement are only mildly manifested during the measurement; a shift to lower temperatures of 5 K and an increase of 0.01 pF in peak height.

Conclusions

The influence of neutron irradiation on minority carrier traps in 4H-SiC was investigated by means of minority carrier transient spectroscopy (MCTS). The spectra revealed three trap levels consequence of the neutron irradiation, labelled as X, B and Y with activation energies of 0.06, 0.22 and 1.6 eV above the valence band edge, respectively. The B level was associated to the B-center found in as-grown SiC, but the peak position was shifted to lower temperatures after a high fluence neutron irradiation. The dynamic behaviour of the traps was also studied. The high defect concentration induced by a neutron fluence of 1×10^{15} cm^{-2} was high enough to compensate the free carriers in the 4H-SiC epi-layers, preventing reliable DLTS measurements and impeding the study of majority carrier traps.

References

[1] J. A. Cooper, M. R. Melloch, R. Singh, A. Agarwal and J. W. Palmour, IEEE Trans. Electron Devices, vol. 49, no. 4, pp. 658-664 (2002).

[2] K. Shenai, K. F. Galloway and R. D. Schrimpf, Int. J. High Speed Electron. Syst., vol. 14, no. 2, pp. 445-463 (2004).

[3] F. Franceschini, F. H. Ruddy, in: *Silicon carbide neutron detectors*, INTECH Open Access Publisher (2011).

[4] C. Martinella, R. G. Alía, R. Stark, A. Coronetti, C. Cazzaniga, M. Kastriotou, Y. Kadi, R. Gaillard, U. Grossner and A. Javanainen, IEEE Transactions on Nuclear Science, vol. 68, no 5, pp. 634-641 (2021).

[5] D.J. Lichtenwalner, B. Hull, E. Van Brunt, S. Sabri, D.A. Gajewski, D. Grider, S. Allen, J.W. Palmour, A. Akturk and J. McGarrity, IEEE International Reliability Physics Symposium pp. 2B.2-1-2B.2-6 (2018).

[6] International Atomic Energy Agency, in *Neutron transmutation doping of silicon at research reactors* (Vienna, 2012).

[7] B. Zippelius, J. Suda and T. Kimoto, Journal of Applied Physics 111(3), 033515 (2012).

[8] N. T. Son, X. T. Trinh, L. S.Løvlie, B. G.Svensson, K.Kawahara, J. Suda, T. Kimoto, T. Umeda, J. Isoya, T. Makino, T. Ohshima, and E. Janzén, Physical Review Letters 109(18), 187603 (2012).

[9] C. Hemmingsson, N. T. Son, O. Kordina, J. P. Bergman, E. Janzén, J. L Lindström, S. Savage and N. Nordell, Journal of Applied Physics 81(9), 6155-6159 (1997).

[10] K. Kawahara, X. Thang Trinh, N. Tien Son, E. Janzén, J. Suda and T. Kimoto, Applied Physics Letters 102(11), 112106 (2013).

[11] G. Alfieri and A. Mihaila, Journal of Physics: Condensed Matter 32(46), 465703 (2020).

[12] M. E. Bathen, A. Galeckas, J. Müting, H. M. Ayedh, U. Grossner, J. Coutinho, Y. K. Frodason and L. Vines, npj Quantum Information 5(1), 1-9 (2019).

[13] S. G. Sridhara, L. L. Clemen, R. P. Devaty, W. J. Choyke, D. J. Larkin, H. S. Kong, T. Troffer, and G. Pensl, Journal of Applied Physics 83, 7909 (1998).

[14] L. Snoj, G. Žerovnik and A. Trkov, Applied Radiation and Isotopes 70(3), 483-488 (2012).

[15] S. Weiss and R. Kassing, Solid-State Electron., vol. 31, no. 12, pp. 1733-1742, Dec. 1988.

[16] D. Menichelli, M. Scaringella, F. Moscatelli, M. Bruzzi and R. Nipoti, Diamond and Related Materials 16(1), 6-11 (2007).

[17] I. Capan, T. Brodara, Y. Yamazakib, Y. Okib, T. Ohshimab, Y. Chibac, Y. Hijikatac, L. Snojd and V. Radulovićd, Nuclear Instruments and Methods in Physics Research Section B: Beam Interactions with Materials and Atoms 478, 224-228 (2020).